Received: 13 July 2022 | Revised: 19 July 2022 | Accepted: 21 July 2022

DOI: 10.1002/jcb.30314

TOOLBOX

Journal of Cellular Biochemistry WILEY

Identification of an ERN1 target site within EGFP mRNA

Marius W. Baeken | **Yohei Yokobayashi**

Nucleic Acid Chemistry and Engineering Unit, Okinawa Institute of Science and Technology Graduate University, Onna, Okinawa, Japan

Correspondence
Yohei Yokobayashi, Nucleic Acid Chemistry and Engineering Unit, Okinawa Institute of Science and Technology Graduate University, Onna, Okinawa 904 0495, Japan.
Email: yohei.yokobayashi@oist.jp

Funding information
Okinawa Institute of Science and Technology Graduate University

Abstract

EGFP (enhanced green fluorescent protein) is one of the most common tools used in life sciences, including research focusing on proteostasis. Here we report that ERN1 (endoplasmic reticulum to nucleus signaling 1), which is upregulated by UPR (unfolded protein response), targets an RNA hairpin loop motif in EGFP mRNA. A silent mutation introduced into EGFP mRNA abolished the ERN1-dependent mRNA decay. Therefore, experiments that employ EGFP as a reporter gene in studies that involve upregulation of the UPR pathway should be interpreted carefully, and a mutant devoid of the ERN1 target motif may be more suitable for such studies.

KEYWORDS
EGFP, ERN1, IRE1, proteostasis, unfolded protein response

1 | INTRODUCTION

The fluorescent protein EGFP (enhanced green fluorescent protein) derived from the green fluorescent protein originally discovered in *Aequorea victoria,* is one of the most commonly used reporters in various disciplines within life sciences. It can be used to observe the localization of fusion proteins within a cell or to monitor the activity of different promoters. Despite its popularity and broad applications, the possibility of EGFP protein or mRNA being differentially targeted by various endogenous posttranscriptional pathways is often overlooked.

One of the many applications of EGFP in life sciences is using a fusion protein consisting of EGFP, mCherry, and MAP1LC3B (microtubule-associated protein 1 light chain 3 beta) to observe autophagic processes within a cell.[1] In this context, BafA1 (Bafilomycin A1) is often employed as a tool to halt autophagosomal fusion with the lysosome.[2] BafA1's modus operandi causes lysosomal lumen deacidification by inhibiting membrane-bound ATPases that supply the lysosome with protons.[3,4] It is implicitly assumed in such experiments that the reporter gene mRNA and protein are not specifically affected by endogenous pathways that are activated by the stimulus such as BafA1.

Like many biological macromolecules, RNAs are subject to degradative processes to recycle their components. Since BafA1 renders the lysosome unable to supply the cell with recycled amino acids and nucleotides, other recycling pathways may be upregulated to compensate. As is the case for the proteasome concerning protein turnover, processes independent of the lysosome may increase RNA turnover. Thus, BafA1 treatment may affect mRNA levels of common reporter proteins. In this work, we report an unexpected targeting of EGFP mRNA by ERN1 (endoplasmic reticulum to nucleus signaling 1) which is upregulated upon BafA1 treatment. We attributed this effect to an RNA motif within the EGFP mRNA recognized by ERN1. Our observation underscores the importance of carefully validating assays based on reporter genes.

2 | MATERIALS AND METHODS

2.1 | Reagents and plasmids

Cell culture media and reagents were obtained from Nacalai Tesque Inc. BafA1 (BIA-B1012; BioAustralis), tunicamycin (35638-74; Nacalai Tesque), and 4μ8C (22110; Cayman Chemical Company) were used without further purification. Oligonucleotides were purchased from Sigma-Aldrich. Recombinant DNase I and SYBR Green I (10 000×) were from Takara Bio. Maxima (H Minus) Reverse Transcriptase was purchased from Thermo Fisher Scientific. pEBFP2-N1 (#54595) and pmOrange-N1 (#54499) plasmids were obtained from Addgene and deposited by Michael Davidson. pEGFP-BsaI and pLuc2-BsaI-Amp were derived from commercial vectors, and their sequences are provided in Supporting Information.

2.2 | Cell culture

HEK-293 cells were cultured following a standard protocol. In brief, cells were cultured in humidified air at 37°C with 5% CO_2, and 20% O_2 in carbonate buffered DMEM with 10% FBS. Cells were never grown past 80% confluency and passaged twice a week. Before the experiments, 0.3×10^6 cells were seeded in six-well plates and left for 24 h in 2.5 ml media. BafA1 with a final concentration of 200 nM in dimethyl sulfoxide (DMSO) was administered 4 h before harvesting. Tunicamycin in DMSO with a final concentration of 500 nM, and 4μ8C with a final concentration of 20 μM in DMSO treatments lasted for 24 h. Controls were treated with 2.5 μl DMSO.

2.3 | Transfection

Exogenous DNA was introduced into HEK-293 cells following the calcium phosphate protocol. Briefly, 1 μg of plasmid DNA was diluted in 105 μl ddH_2O and 15 μl 2 M $CaCl_2$. To this solution 120 μl of phosphate buffer (280 mM NaCl, 50 mM HEPES, 1.5 mM Na_2HPO_4; pH 7.12) was carefully added dropwise. After incubation for 30 min, the solution was dropwise added to cells cultured in 2.5 ml medium in six-well plates. After 24 h, the old medium was discarded, and the cells were washed once with medium and cultured for additional 24 h. After washing the cells with 1×PBS, cellular fluorescence was measured using the Infinite M1000 PRO microplate reader from Tecan. Untransfected cells were used as blank. EGFP (488 nm/507 nm), EBFP2 (383 nm/448 nm), and mOrange (538 nm/562 nm) fluorescence was normalized on mCherry (587 nm/610 nm) fluorescence.

2.4 | qPCR

Total RNA was harvested from the transfected HEK-293 cells using the RNeasy Mini kit from Qiagen. Contaminating DNA was removed by incubation with recombinant DNase I for 30 min at 37°C. cDNA was synthesized using an oligo-dT primer with the Maxima (H Minus) Reverse Transcriptase, following the manufacturer's instructions with 1 μg total RNA as input. qPCRs were done using OneTaq 2xMasterMix with primers (500 nM) and 1×SYBR Green I over a total of 40 cycles using the following cycling program: 95°C 10 min, (95°C 30 s, 60°C 1 min, 68°C 1 min) × 39 cycles. The following primers were used (for/rev in 5′-3′): EGFP (CAGCGTGTCCG GC/GGCTGAAGCACTGCAC), EBFP2 (CAGCGTGAGG GGC/GGCGAAGCACTGCAC), mOrange (TCTCTTCAC CTACGGCTCCAA/CTTGACCTCGGAGGTGTAGTG), mCherry (TCAGTTCATGTACGGCTCCAAG/TTGAC CTCAGCGTCGTAGTG), Luc2 (CGCACATATCGAGG TGGACA/GCAAGCTATTCTCGCTGCAC), XBP1spliced (GCTGAGTCCGCAGCAGGT/CTGGGTCCAAGTTGTCC AGAAT), XBP1unspliced (CAGACTACGTGCACCTCT GC/CTGGGTCCAAGTTGTCCAGAAT), XBp1total (TGA AAAACAGAGTAGCAGCTCAGA/CCCAAGCGCTGTCT TAACTC), and RPL19 (CTCGATGCCGGAAAAACACC/ TGACCTTCTCTGGCATTCGG).

2.5 | Sequence alignment

Sequence alignment was performed ClustalOmega[5] with sequences of EGFP, EBFP2, mCherry, mOrange, and annotated sequences of cnidarian GFP-like proteins.

2.6 | Microscopy

EGFP and mCherry fluorescence images in Figure 2 and Figure 3 were documented in live wells using a T2-Eclipse system from Nikon with x10 magnification. Images in Figure 1 were recorded using an A1R system from Nikon with x40 magnification.

2.7 | Statistics

Graphs and statistics were assembled using GraphPad Prism 9 from GraphPad Software, Inc. Two-way analysis

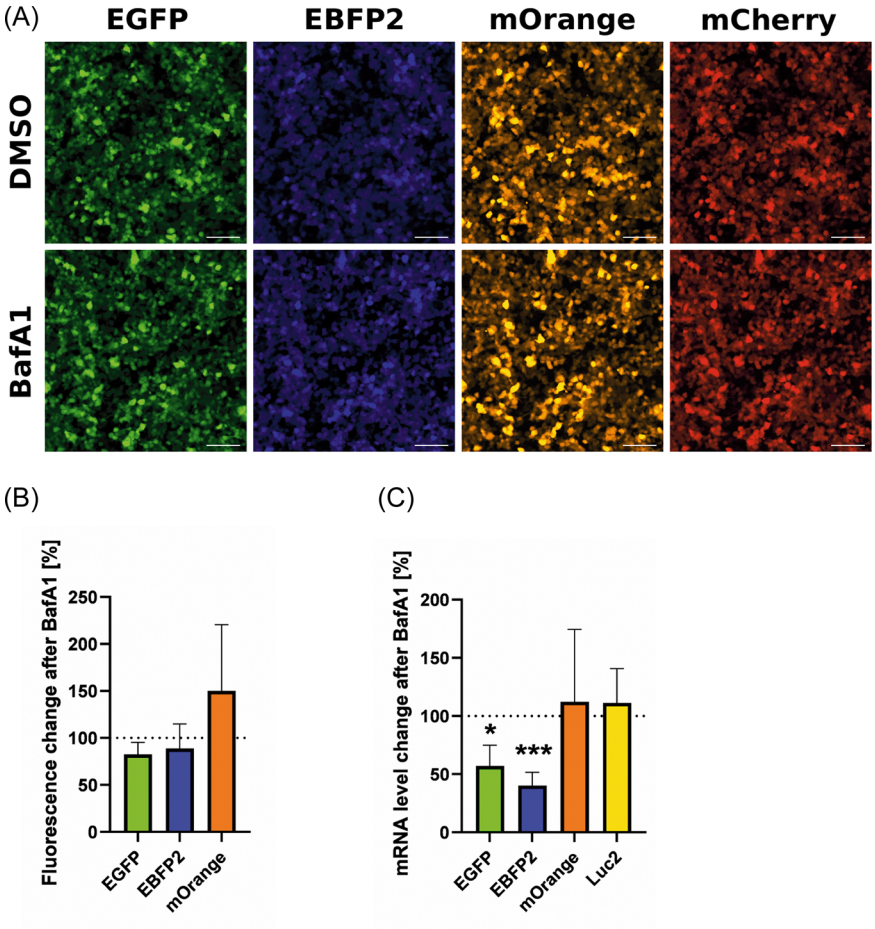

FIGURE 1 BafA1 treatment affects EGFP mRNA levels. (A) Representative fluorescence images of the transfected HEK-293 cells after 4 h treatments with DMSO or BafA1. Scale bars represent 100 μm. (B) Changes in fluorescence of the cells transfected with EGFP, EBFP2, and mOrange plasmids normalized by mCherry fluoresence upon BafA1 treatment measured by plate reader ($n = 3$). (C) Changes in the levels of EGFP, EBFP2, mOrange, and Luc2 mRNAs normalized by mCherry mRNA level upon BafA1 treatment ($n = 5$). "*" indicates significant differences compared to the DMSO treated control group. The symbol number indicates the grade of significance with $*p < 0.05$. BafA1, Bafilomycin A1; DMSO, dimethyl sulfoxide; EGFP, enhanced green fluorescent protein.

of variance followed by an original Benjamini and Hochberg posthoc tests were applied.

3 | RESULTS

3.1 | BafA1 treatment triggers mRNA turnover of fluorescent proteins

First, we ectopically overexpressed various fluorescent proteins (EGFP, EBFP2, mOrange, mCherry) in HEK-293 cells and assessed their fluorescence levels. We employed mCherry as the transfection control due to its high stability, also under conditions of proteostatic stress.[6,7] After 4 h of treatment with 200 nM BafA1, we did not observe significant changes in the fluorescence intensities of any protein (Figure 1A,B).

Next, we looked at their mRNA levels (Figure 1C). Here, we found that the mRNA levels of EGFP and EBFP2 normalized by that of mCherry significantly decreased upon BafA1 treatment, while the mRNA levels of mOrange and the firefly luciferase, Luc2, remained stable. Since the ORFs of EGFP and EBFP2, or mOrange and mCherry are highly similar, we examined whether the used primers would yield nonspecific amplicons. The expected amplicons were 136 bp for EGFP/EBFP2 and 345 bp for mOrange/mCherry. PCRs mirroring the conditions of the qPCR protocol using plasmids as templates showed little to no nonspecific products (Supporting Information: Figure S1). Therefore, it appears that mRNAs of EGFP and EBFP2 are specifically downregulated upon BafA1 treatment.

3.2 | Mutation of a CAGCAG loop motif stabilizes EGFP mRNA in BafA1 treated cells

Observations above led us to consider various physiological consequences of BafA1 treatment that may differentially regulate the reporter mRNAs. Since lysosomal dysfunction would affect the general nucleotide supply, other mechanisms to degrade RNA may be upregulated. However, increased exonuclease activity would seem unlikely since the untranslated regions of the EGFP, EBFP2, mOrange, and mCherry mRNAs are highly similar.

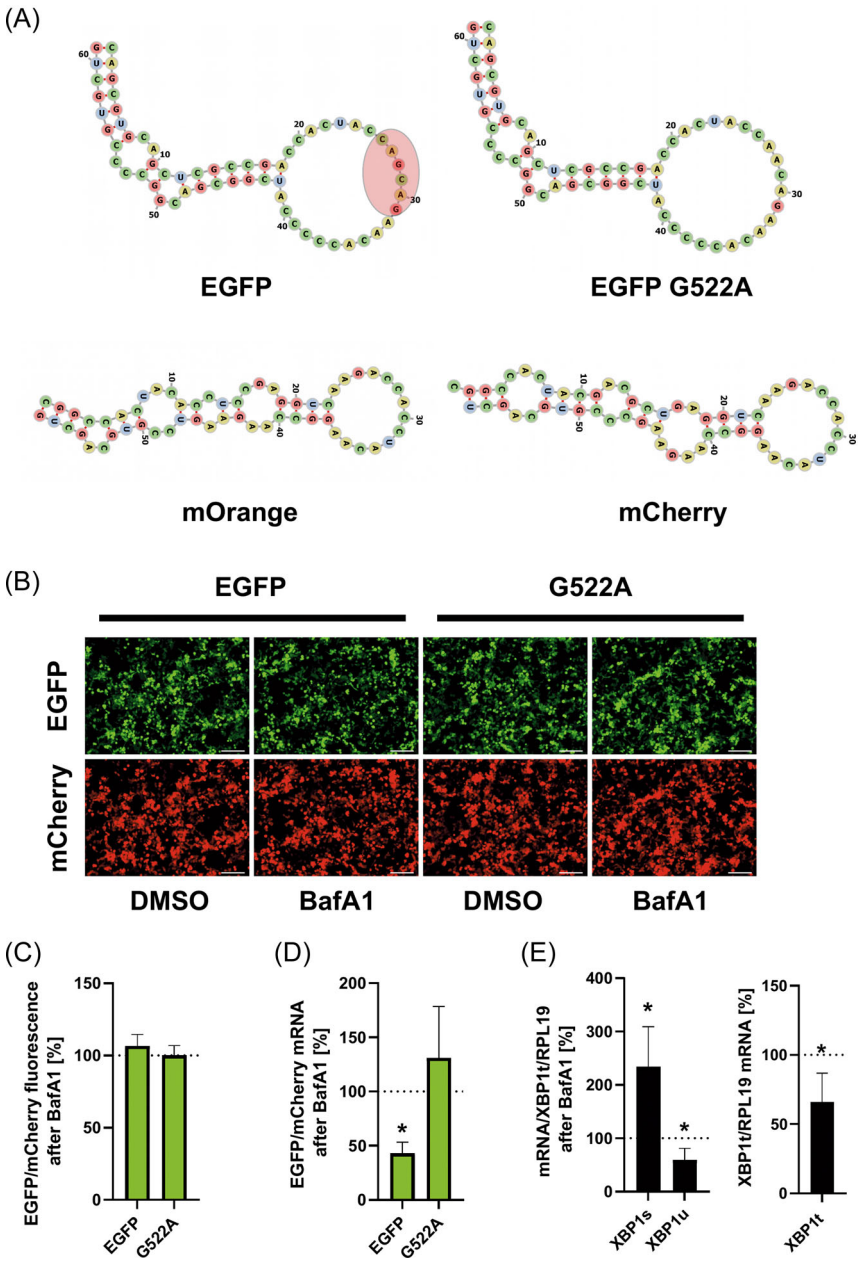

FIGURE 2 EGFP mRNA is targeted by ERN1 induced by BafA1. (A) Illustration of the stem-loop structure in the EGFP mRNA displaying a putatuve ERN1 target side (red circle), and the homologous regions in the mOrange and mCherry mRNAs. The secondary structure was predicted using RNAfold web server.[25] (B) Representative fluorescence images of the HEK-293 cells transfected with EGFP and $EGFP^{G552A}$ expressing plasmids after 4 h treatments with DMSO or BafA1. mCherry plasmid was cotransfected as a control. Scale bars represent 200 μm. (C) Changes in fluorescence of the cells transfected with EGFP and $EGFP^{G552A}$ plasmids normalized by mCherry fluoresence upon BafA1 treatment measured by plate reader ($n = 3$). (D) Changes in the levels of EGFP and $EGFP^{G552A}$ mRNAs normalized by mCherry mRNA level upon BafA1 treatment ($n = 3$). (E) Changes in XBP1 mRNA levels normlaized by RPL19 mRNA level upon BafA1 treatment. The left graph shows regulation of the splice variants produced by ERN1 activity, and the right graph shows regulation of total XBP1 mRNA. "*" indicates significant differences compared to the DMSO treated control group. The symbol number indicates the grade of significance with $*p < 0.05$. BafA1, Bafilomycin A1; DMSO, dimethyl sulfoxide; EGFP, enhanced green fluorescent protein; ERN1, endoplasmic reticulum to nucleus signaling 1.

Therefore, we decided to focus on the endogenous endonuclease ERN1 which is intimately integrated into the UPR (unfolded protein response) signaling.[8] Indeed, previous studies reported that ERN1 mRNA levels increased after BafA1 treatments.[9] Interestingly, a closer look at the mRNAs of EGFP and EBFP2 revealed a stem-loop presenting a nucleotide sequence (CAGCAG) (Figure 2A), which resembles a potential target site for

ERN1.[10] In EGFP mRNA, this sequence encodes two consecutive glutamine residues.

The putative ERN1 target site was destroyed by replacing the 552nd base of EGFP's coding sequence with an adenine (CAACAG). This mutation does not alter the encoded amino acid, and it is unlikely to disturb the local mRNA structure (Figure 2A). The corresponding regions of the mRNAs encoding mOrange and mCherry do not contain consecutive glutamine-coding codons and are not predicted to fold into similar structures (Figure 2A).

Neither EGFP nor its EGFP^{G552A} mutant showed change in fluorescence after 4 h of BafA1 treatment (Figure 2B,C). The mutation did not affect fluorescence intensity of the transfected cells (Figure 2B). However, the mRNA level of EGFP^{G552A} did not show a significant change upon BafA1 treatment, while the original EGFP mRNA level decreased by ~50% (Figure 2D).

Data concerning BafA1's ability to trigger UPR, although reported, can be considered somewhat limited.[9] Therefore, we also wanted to verify whether BafA1 indeed induced ERN1 activity. XBP1 (X-box binding protein 1) mRNA is a well-described and well-conserved target for ERN1. During UPR, XBP1 mRNA is cleaved at two positions by ERN1, which results in an alternatively spliced variant of XBP1.[11] Using published primer sequences,[11] we analyzed the splicing status of XBP1 transcripts per the amount of total transcripts via qPCR. Following BafA1 treatment, the spliced isoform of XBP1 increased significantly, while the fraction of unspliced XBP1 transcripts significantly decreased (Figure 2E). Interestingly, we could also observe a significant reduction of total XBP1 transcription (Figure 2E). RPL19 (60S ribosomal protein L19) was used for normalization.

3.3 | The G552A mutant is resistant to ERN1-dependent degradation

Next, we were interested whether we could observe relevant improvements using the ERN1-resistant EGFP^{G552A} in the context of proteostasis. Therefore, we treated cells with tunicamycin to strongly induce the UPR and ERN1 activity.[12] Moreover, we used 4μ8C to inhibit ERN1's endonucleolytic activity.[13]

In contrast to BafA1 treatment, cells treated with 500 nM tunicamycin for 24 h showed significantly reduced EGFP fluorescence. As expected, this effect could be prevented by simultaneous treatment with 20 μM 4μ8C (Figure 3A,B). Furthermore, this effect did not persist in EGFP^{G552A}, indicating that more EGFP was translated due to decreased mRNA turnover. 4μ8C treatment itself did not alter EGFP fluorescence.

The mRNA levels of EGFP and EGFP^{G552A} followed a similar pattern. Tunicamycin had no effect on the mRNA level of EGFP^{G552A} suggesting that it is resistant to ERN1-dependent degradation (Figure 3C). Overall, we can conclude that ERN1 exerts endonucleolytic activity toward the mRNA of conventional EGFP.

3.4 | Sequencing alignment of EGFP and other fluorescent proteins

Like many other tools in molecular biology, EGFP's coding sequence was codon-optimized for expression in mammalian cells. Out of the two codons that code for glutamine, CAG is considered to be optimal in mammals.[14] Thus, we decided to briefly look at the homologous sequences from EGFP orthologues from different species (Figure 3D).

A. victoria GFP, from which EGFP was engineered, contains CAACAA at the same region. Interestingly, organisms that have conserved one or both glutamines do not contain the tandem CAG motif. Therefore, the CAGCAG motif in EGFP was most likely introduced unintentionally during codon optimization.

4 | DISCUSSION

Fluorescent proteins, with EGFP being the most prominent, have become common and crucial tools in life sciences. They are used as marker proteins for cell sorting and flow cytometry, as fusion proteins to study protein localization, as readouts to study promoter activity, and for countless other purposes.[15–17] Autophagy is no exception since fluorescent proteins have been used as a cargo protein to study autophagic activity or as a complex fusion protein that enables visual distinction between autophagosomes and autophagolysosomes.[1,18]

Many of these applications implicitly assume that EGFP and other fluorescent proteins are not selectively targeted by various cellular pathways. Our results indicate that we still have not discovered everything concerning these common tools. Proteostatic stress, which induces ERN1 activity, is often used as a tool in many different research areas, not just autophagy. Many disease models, for example, the Alzheimer's disease models focusing on Tau hyperphosphorylation or Parkinson's disease models based on alpha-synuclein aggregation, are intertwined with proteostatic events by design.[19–22] Since EGFP is also often used in these contexts, the possibility of ERN1 influencing, for example, fusion proteins, should be considered. As our data indicate, for experiments that employs tunicamycin,

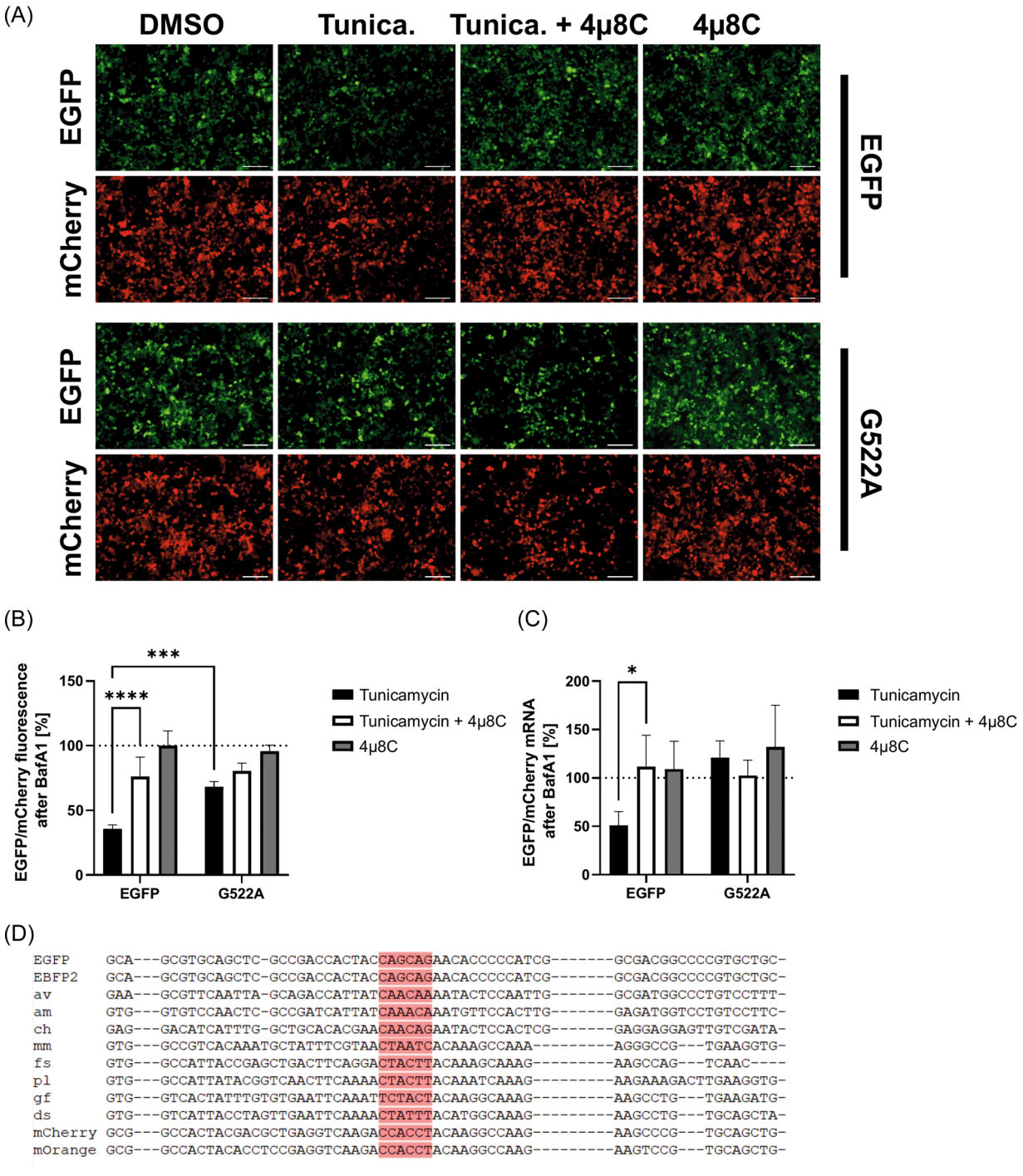

FIGURE 3 Mutation of the ERN1 target motif in EGFP mRNA. (A) Representative fluorescence images of the HEK-293 cells transfected with EGFP and EGFP^{G552A} after 24 h treatment with DMSO or tunicamycin and/or 4μ8C. Scale bars represent 200 μm. (B) Changes in fluorescence of the cells transfected with EGFP and EGFP^{G552A} plasmids normalized by mCherry fluoresence upon treatment with tunicamycin, tunicamycin + 4μ8C, or 4μ8C measured by plate reader ($n = 3$). (C) Changes in the levels of EGFP and EGFP^{G552A} mRNAs normalized by mCherry mRNA level upon treatment with tunicamycin, tunicamycin + 4μ8C, or 4μ8C ($n = 3$). "*" indicates significant differences compared to the DMSO treated control group. The symbol number indicates the grade of significance with *$p < 0.05$, ***$p < 0.001$, ****$p < 0.0001$. (D) Alignment of the genes encoding GFP-like proteins from different cnidarians. The CAGCAG motif and its homologs are highlighted in red. am, *Aldersladia magnificus*; av, *Aequorea victoria;* ch, *Clytia hemisphaerica;* ds, *Discosoma striata*; DMSO, dimethyl sulfoxide; EGFP, enhanced green fluorescent protein; ERN1, endoplasmic reticulum to nucleus signaling 1; fs, *Fungia scutaria;* gf, *Galaxea fascicularis;* mm, *Meandrina meandrites;* pl, *Porites lobata.*

for example, EGFP^{G552A} may produce more robust results than the original EGFP.

Considering that EGFP protein has a half-life of approximately 26 h,[23] differences between EGFP and EGFP^{G552A} may not be conspicuous in short experiments such as those described in this work. However, protein accumulation may be affected more significantly by ERN1 targeting in experiments of longer time scale, or when a destabilized form of EGFP with a reduced half-life of 5.5 h[24] is used.

In summary, we would highly recommend keeping possible side effects of proteostatic stress on EGFP mRNA levels in mind, especially in the context of autophagy, where BafA1 is one of the most common tools used to inhibit autophagosomal fusion. Using EGFP^{G552A} may be more suitable for these kinds of assays in the future.

AUTHOR CONTRIBUTIONS

Marius W. Baeken designed experiments, analyzed data, and wrote the manuscript. Yohei Yokobayashi supervised experiments, analyzed data, and edited the manuscript.

ACKNOWLEDGMENTS

We would like to express our gratitude toward Paolo Barzaghi from the OIST imaging section for his assistance with the confocal microscope. This work was funded by OIST.

CONFLICT OF INTEREST

The authors declare no conflict of interest.

DATA AVAILABILITY STATEMENT

The data that support the findings of this study are available from the corresponding author upon reasonable request.

ORCID

Yohei Yokobayashi http://orcid.org/0000-0002-2417-1934

REFERENCES

1. Kimura S, Noda T, Yoshimori T. Dissection of the autophagosome maturation process by a novel reporter protein, tandem fluorescent-tagged LC3. *Autophagy*. 2007;3:452-460. doi:10.4161/auto.4451
2. Klionsky DJ, Abdelmohsen K, Abe A, et al. Guidelines for the use and interpretation of assays for monitoring autophagy (3rd edition). *Autophagy*. 2016;12(1):1-222. doi:10.1080/15548627.2015.1100356
3. Trivedi PC, Bartlett JJ, Pulinilkunnil T. Lysosomal biology and function: modern view of cellular debris bin. *Cells*. 2020;9(5):1131. doi:10.3390/cells9051131
4. Wang R, Wang J, Hassan A, et al. Molecular basis of V-ATPase inhibition by bafilomycin A1. *Nat Commun*. 2021;12(1):1782. doi:10.1038/s41467-021-22111-5
5. Madeira F, Pearce M, Tivey ARN, et al. Search and sequence analysis tools services from EMBL-EBI in 2022. *Nucleic Acids Res. gkac240*. 2022;50(W1):W276-W279. doi:10.1093/nar/gkac240
6. Pankiv S, Clausen TH, Lamark T, et al. p62/SQSTM1 binds directly to Atg8/LC3 to facilitate degradation of ubiquitinated protein aggregates by autophagy. *J Biol Chem*. 2007;282(33):24131-24145. doi:10.1074/jbc.M702824200
7. Mustafina K, Fukunaga K, Yokobayashi Y. Design of mammalian ON-riboswitches based on tandemly fused aptamer and ribozyme. *ACS Synth Biol*. 2020;9(1):19-25. doi:10.1021/acssynbio.9b00371
8. Yoshida H, Matsui T, Yamamoto A, et al. XBP1 mRNA is induced by ATF6 and spliced by IRE1 in response to ER stress to produce a highly active transcription factor. *Cell*. 2001;107(7):881-891. doi:10.1016/s0092-8674(01)00611-0
9. Kawaguchi T, Miyazawa K, Moriya S, et al. Combined treatment with bortezomib plus bafilomycin A1 enhances the cytocidal effect and induces endoplasmic reticulum stress in U266 myeloma cells: crosstalk among proteasome, autophagy-lysosome and ER stress. *Int J Oncol*. 2011;38(3):643-654. doi:10.3892/ijo.2010.882
10. Maurel M, Chevet E, Tavernier J, Gerlo S. Getting RIDD of RNA: IRE1 in cell fate regulation. *Trends Biochem Sci*. 2014;39(5):245-254. doi:10.1016/j.tibs.2014.02.008
11. Yoon SB, Park YH, Choi SA, et al. Real-time PCR quantification of spliced X-box binding protein 1 (XBP1) using a universal primer method. *PLoS One*. 2019;14(7):e0219978. doi:10.1371/journal.pone.0219978
12. Hetz C, Papa FR. The unfolded protein response and cell fate control. *Mol Cell*. 2018;69(2):169-181. doi:10.1016/j.molcel.2017.06.017
13. Oh-Hashi K, Kohno H, Kandeel M, Hirata Y. Characterization of IRE1α in Neuro2a cells by pharmacological and CRISPR/Cas9 approaches. *Mol Cell Biochem*. 2020;465(1-2):53-64. doi:10.1007/s11010-019-03666-w
14. Hiss M, Schneider L, Grosche C, et al. Combination of the endogenous lhcsr1 promoter and codon usage optimization boosts protein expression in the moss *Physcomitrella patens*. *Front Plant Sci*. 2017;8:1842. doi:10.3389/fpls.2017.01842
15. Galbraith DW, Anderson MT, Herzenberg LA. Flow cytometric analysis and FACS sorting of cells based on GFP accumulation. *Methods Cell Biol*. 1999;58:315-341. doi:10.1016/s0091-679x(08)61963-9
16. Kanda T, Sullivan KF, Wahl GM. Histone-GFP fusion protein enables sensitive analysis of chromosome dynamics in living mammalian cells. *Curr Biol*. 1998;8(7):377-385. doi:10.1016/s0960-9822(98)70156-3
17. Wang P, Nolan TM, Yin Y, Bassham DC. Identification of transcription factors that regulate ATG8 expression and autophagy in Arabidopsis. *Autophagy*. 2020;16(1):123-139. doi:10.1080/15548627.2019.1598753
18. Larsen KB, Lamark T, Øvervatn A, et al. A reporter cell system to monitor autophagy based on p62/SQSTM1. *Autophagy*. 2010;6(6):784-793. doi:10.4161/auto.6.6.12510
19. Nijholt DA, van Haastert ES, Rozemuller AJ, et al. The unfolded protein response is associated with early tau

pathology in the hippocampus of tauopathies. *J Pathol*. 2012;226(5):693-702. doi:10.1002/path.3969

20. El Manaa W, Duplan E, Goiran T, et al. Transcription- and phosphorylation-dependent control of a functional interplay between XBP1s and PINK1 governs mitophagy and potentially impacts Parkinson disease pathophysiology. *Autophagy*. 2021;17(12):4363-4385. doi:10.1080/15548627.2021
21. Kataura T, Tashiro E, Nishikawa S, et al. A chemical genomics-aggrephagy integrated method studying functional analysis of autophagy inducers. *Autophagy*. 2021;17(8):1856-1872. doi:10.1080/15548627.2020.1794590
22. Ghemrawi R, Khair M. Endoplasmic reticulum stress and unfolded protein response in neurodegenerative diseases. *Int J Mol Sci*. 2020;21(17):6127. doi:10.3390/ijms21176127
23. Corish P, Tyler-Smith C. Attenuation of green fluorescent protein half-life in mammalian cells. *Protein Eng*. 1999;12(12):1035-1040. doi:10.1093/protein/12.12.1035
24. Kitsera N, Khobta A, Epe B. Destabilized green fluorescent protein detects rapid removal of transcription blocks after genotoxic exposure. *Biotechniques*. 2007;43(2):222-227. doi:10.2144/000112479
25. Gruber AR, Lorenz R, Bernhart SH, et al. The Vienna RNA websuite. *Nucleic Acids Res*. 2008;36(suppl 2):W70-W74. doi:10.1093/nar/gkn188

SUPPORTING INFORMATION

Additional supporting information can be found online in the Supporting Information section at the end of this article.

How to cite this article: Baeken MW, Yokobayashi Y. Identification of an ERN1 target site within EGFP mRNA. *J Cell Biochem*. 2022;1-8. doi:10.1002/jcb.30314